A Satellite View of the Radiative Impact of Clouds on Surface Downward Fluxes in the Tibetan Plateau

C. M. NAUD

Department of Applied Physics and Applied Mathematics, Columbia University, New York, New York

I. RANGWALA

Western Water Assessment, University of Colorado, and NOAA/ESRL/Physical Sciences Division, Boulder, Colorado

M. XU

Department of Ecology, Evolution and Natural Resources, Rutgers, The State University of New Jersey, New Brunswick, New Jersey

J. R. MILLER

Institute of Marine and Coastal Science, Rutgers, The State University of New Jersey, New Brunswick, New Jersey

(Manuscript received 17 July 2014, in final form 27 October 2014)

ABSTRACT

Using 13 yr of satellite observations for the Tibetan Plateau, the sensitivities (or partial derivatives) of daytime surface downward shortwave and longwave fluxes with respect to changes in cloud cover and cloud optical thickness are investigated and quantified. Coincident cloud and surface flux retrievals from the NASA Moderate Resolution Imaging Spectroradiometer and the Clouds and the Earth's Radiant Energy System, respectively, as well as ground-based observations at 11 stations across the plateau are used to examine the spatial and seasonal variability of this sensitivity over the entire plateau. The downward shortwave flux is found to be modulated primarily by changes in cloud cover, but changes in optical thickness also have an impact, as revealed by a multiple regression fit. The coefficient of determination of the regression increases by more than 15% when optical thickness is added. There is significant seasonal and regional variability in the cloud radiative impact. On average, at all stations, the sensitivity of surface shortwave flux to changes in cloud cover is about $-0.5 \pm 0.1\,\mathrm{W\,m^{-2}\,\%^{-1}}$ in winter according to both ground-based and satellite observations but in summer reaches -1.5 ± 0.3 and $-1.8 \pm 0.2\,\mathrm{W\,m^{-2}\,\%^{-1}}$ according to ground-based and satellite observations, respectively. Cloud cover itself has little impact on the sensitivity when clouds are optically thin, but above an optical thickness of 12, sensitivities increase with both cloud cover and cloud optical thickness. The daytime longwave flux response to changes in cloud properties is also examined. The radiative impact of a decrease in cloud cover on the surface net flux can be offset or even canceled if cloud opacity increases by 5%–10%.

1. Introduction

The Tibetan Plateau, often referred to as the third pole, provides freshwater to one of the most populated regions in the world. Its climate influences the general circulation of the atmosphere and thus the Asian monsoon system (e.g., Yanai et al. 1992; Ye and Wu 1998). It is paramount in evaluating how climate change may affect this region where evidence is mounting for enhanced warming rates in this area relative to the global or Chinese averages (e.g., Liu and Chen 2000; Liu et al. 2004; Wang et al. 2008; Pepin and Lundquist 2008). Furthermore, climate models project significant warming trends in this region during the twenty-first century (e.g., Rangwala et al.

Corresponding author address: Catherine Naud, 2880 Broadway, New York, NY 10025.
E-mail: cn2140@columbia.edu

DOI: 10.1175/JAMC-D-14-0183.1

2013). One critical and relatively difficult question to address is the role of clouds in influencing enhanced surface temperature responses in this region.

During the latter half of the twentieth century, a decreasing trend in surface insolation (dimming) was found globally (Wild 2009 and reference therein) and in particular in China (Kaiser and Qian 2002; Qian et al. 2006; Xia 2010). However, during the last two decades, a global reversal of this trend (brightening) has been observed (Wild 2009), albeit not so clearly for China (Xia 2010). These trends in dimming and brightening have been attributed to atmospheric aerosols but for the Tibetan Plateau region the observations are much more limited and our understanding of these trends and their causes less clear.

Duan and Wu (2006) reported changes in cloud amount over the Tibetan Plateau [also identified by Zhang et al. (2008) and Yang et al. (2012)] and suggested that these changes (i.e., daytime decrease, nighttime increase) played a role in the temperature increase in the region, through their radiative impact. Ye et al. (2009), for example, found a strong correlation between surface downward shortwave fluxes and the diurnal temperature range. Yang et al. (2012) demonstrated that the increase in deep convective cloud occurrence can explain the decrease in cloud cover (CC), but also the decrease in surface flux as cloud optical thickness τ has increased. They claim that this effect is more important than the observed changes in aerosols in this region. Their study suggests that cloud amount alone is not sufficient to explain the influence of cloud variability on surface flux changes over the Tibetan Plateau. While the findings of Duan and Wu (2006) or Yang et al. (2012) suggest the importance of clouds in the climatology of the Tibetan Plateau, they also reveal how difficult it is to quantify their impact. Both studies rely on ground-based observations (GB) from meteorological and research stations to analyze trends. These stations are mostly found in the more populated regions of the eastern part of the plateau and only report cloud cover, lacking the capabilities to provide information on cloud optical properties.

In this study, we expand on the previous work described above by exploring the impact of changes in cloud cover and optical thickness on the surface shortwave and daytime longwave downward radiation in the Tibetan Plateau region. We use 13 yr of coincident satellite-derived radiation and cloud data from the NASA Clouds and the Earth's Radiant Energy System (CERES; Wielicki et al. 1996; Smith et al. 2011) and Moderate Resolution Imaging Spectroradiometer (MODIS; Salomonson et al. 1989). These datasets allow us to explore a larger area of the plateau than did previous studies and, in particular, the more remote central and western regions. Also, by adding cloud optical thickness, we can examine the concomitant impacts of this cloud property with the more readily available cloud cover on both shortwave and longwave fluxes, measurements that are also scarce in this region. Satellite estimates of surface fluxes may exhibit large uncertainties in this region (e.g., Yang et al. 2008) and retrievals of cloud cover also have their limitations (e.g., Naud and Chen 2010). To test the quality of these datasets, we use ground measurements of cloud cover and shortwave flux from 11 stations scattered across the Tibetan Plateau and surrounding regions (Fig. 1). Using MODIS and CERES data, along with the ground observations, we estimate the change in downward shortwave and daytime longwave fluxes for a given change in both cloud cover and optical thickness. Furthermore, we quantify the spatial and seasonal changes in surface downward fluxes as a function of changes in cloud cover and optical thickness.

2. Data and methodology

Our region of interest extends from 80° to 104°E and from 25° to 40°N and fully includes the Tibet–Qinghai Plateau (Fig. 1). The MODIS and CERES instruments are both available on two distinct polar-orbiting platforms, *Terra* (launched in 1999) and *Aqua* (launched in 2002), that have equator-crossing times 3 h apart (~1030 and 1330 local time). On average, at these latitudes, *Terra* and *Aqua* provide four distinct observations of coincident cloud and derived surface fluxes per day, two of which are during the daytime. We analyze the entire period of observations from 2000 to 2012 (at the time of this analysis, CERES 2013 fluxes were not fully processed).

a. *Description of the datasets*

The level-3 daily surface radiative fluxes from CERES are provided as a combination of *Terra* and *Aqua* retrievals and are available as a global 1° × 1° gridded product in the "SYN1deg Ed3A" files (Wielicki et al. 1996; Doelling et al. 2013). Prior to the *Aqua* launch in 2002, only *Terra* observations are used. Because CERES can only measure top-of-the-atmosphere fluxes, the CERES surface fluxes are calculated with a radiative transfer model using atmospheric profiles provided by the Global Modeling and Assimilation Office and MODIS-derived cloud and aerosol properties (e.g., Smith et al. 2011; Kato et al. 2011, 2013). These calculations are then constrained by the observed top-of-the-atmosphere outgoing fluxes and assume a fixed top-of-the-atmosphere insolation. To obtain daily retrievals that take into account the diurnal changes in fluxes, geostationary satellite radiances and cloud properties are used to correct for the irregular time sampling of the instrument. The MODIS-derived cloud properties used by the CERES team (Minnis et al. 2011)

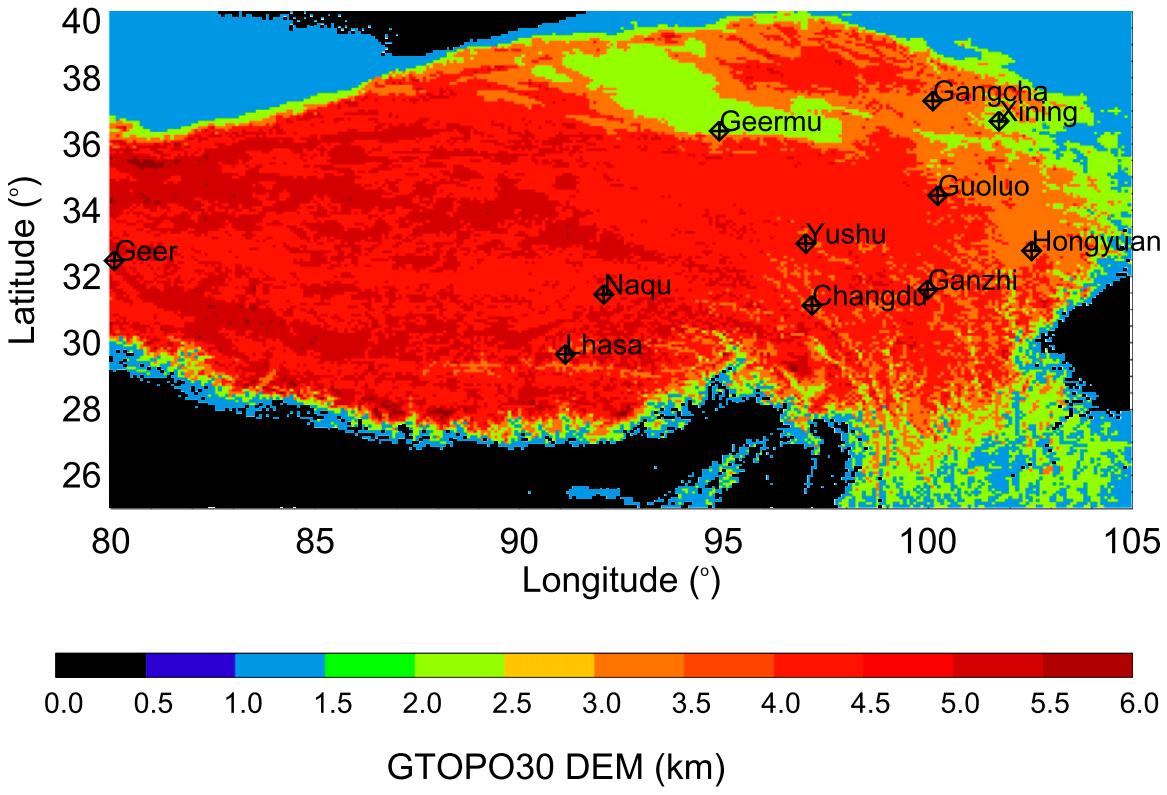

FIG. 1. Elevation map of the Tibetan Plateau and surrounding regions, with locations of research stations indicated by plus signs inside diamonds (see Table 1). The elevations were obtained from the GTOPO30 digital elevation model of the U.S. Geological Survey.

are not from the same algorithms as are used in the operational MODIS cloud products that we describe and use below. As such, there is some degree of independence between the flux estimates and cloud properties. More information on the SYN1deg products can also be found in the CERES data quality summary on the NASA website (available at http://ceres.larc.nasa.gov/products.php?product=SYN1deg). Based on the work of Kato et al. (2012), we expect the uncertainty in the estimated shortwave surface flux to be on the order of 15 W m^{-2} in this region of varying elevations. We expect the uncertainty to be larger in regions of highly variable elevations (e.g., the Himalayas) than in less variable elevation regions (e.g., the central part of the plateau), based on the work of Yang et al. (2008). To obtain daytime-only daily averages of the surface downward longwave flux, we use instead 3-hourly SYN1deg files and averaged the longwave flux for the 3-hourly time steps that have a nonzero shortwave flux. Surface longwave fluxes may be overestimated in dry-arid regions (see the CERES data quality summary).

The *Terra* and *Aqua* MODIS level-3 daily mean cloud cover is also available on a global 1° × 1° grid based on the 1-km-resolution MODIS cloud mask (Ackerman et al. 2008). The data product version is collection 5.1 (the new version 6 is still being processed at the time of this study). We average together data from the two platforms from 2002 onward. Prior to the *Aqua* launch in 2002, the MODIS daily cloud cover is only obtained from *Terra*. We use the daytime and nighttime cloud cover and daytime optical thickness products (Platnick et al. 2003). MODIS cloud cover is known to be underestimated when cloud optical thickness is less than 0.4 (Ackerman et al. 2008) or overestimated when the instrument scan angle is large (Minnis 1989; Zhao and Di Girolamo 2004; Ackerman et al. 2008). Passive instruments tend to underestimate cloud detections over snow-covered land but this is a predominantly nighttime issue (e.g., Naud and Chen 2010) and should not affect our examination of cloud impact on the daytime surface fluxes.

Ground-based observations of cloud amount and surface downward shortwave flux for 2000–05 were obtained for 11 research stations across the Tibetan Plateau. Figure 1 and Table 1 give the locations and names of these stations. According to Shi et al. (2008), the fluxes are measured since the 1990s with a Chinese-made DFY-4 pyranometer, and the expected accuracy is within 5%. Cloud cover is estimated by ground observers, and given as the total and low cloud cover in deciles, which we converted into a percentage. We could

TABLE 1. Comparison between GB and CERES surface downward SW flux and MODIS CC at 11 stations across the Tibetan Plateau: mean and standard deviation (std dev) of the daily difference and R^2. Ge'ermu and Guoluo are also sometimes referred to as Golmud and Dawu, respectively.

Station (lat, lon)	Mean GB minus CERES flux ($W\,m^{-2}$)	Std dev of GB minus CERES flux ($W\,m^{-2}$)	R^2 of GB vs CERES flux	Mean GB minus MODIS CC (%)	Std dev of GB minus MODIS CC (%)	R^2 of GB vs MODIS CC
Lhasa (29.67°N, 91.13°E)	−60	24	0.8	2	18	0.7
Gangcha (37.33°N, 100.13°E)	−42	29	0.8	−3	27	0.5
Ge'ermu (36.42°N, 94.9°E)	−64	23	0.9	8	31	0.3
Xining (36.72°N, 101.75°E)	−59	26	0.9	4	25	0.6
Ge'er (32.5°N, 80.08°E)	−62	28	0.9	−8	21	0.6
Naqu (31.48°N, 92.07°E)	−56	33	0.7	−3	21	0.6
Yushu (33.02°N, 97.02°E)	−68	34	0.8	1	25	0.5
Guoluo (34.47°N, 100.25°E)	−43	28	0.8	1	24	0.5
Changdu (31.15°N, 97.17°E)	−64	32	0.7	−5	21	0.6
Ganzhi (31.62°N, 100°E)	−52	33	0.7	−4	21	0.6
Hongyuan (32.80°N, 102.55°E)	−49	36	0.7	−2	21	0.6

only obtain *daily* averages of the surface downward shortwave flux and cloud cover (longwave flux is not available). The daily cloud cover is the average of all observations performed by a ground observer during a day, usually four equally spaced occurrences during the 24-h period. This means that nighttime cloud cover is included in the daily cloud cover data and cannot be removed from the daily means. Consequently, if the station experiences a noticeable diurnal cycle, or if atmospheric conditions change rapidly within a day, the daily mean of the cloud cover may differ significantly from the daytime mean of the cloud cover that actually impacts the downward shortwave flux. Also, ground observers can miss cirrus or altostratus clouds at night (e.g., Warren et al. 1985), which can cause an underestimate in the daily average cloud cover (Kaiser 1998). Consequently, some error in the relationship between the ground-based downward shortwave flux and cloud cover is expected.

b. Methodology

Because the length of day changes with season, the daily shortwave flux includes a strong seasonal signal that can obscure the modulation in flux caused by changes in cloud properties. To resolve this issue, we examine the deviation of these daily fluxes from their day-of-year mean instead of the actual daily fluxes. We estimate this quantity by first averaging the 2000–12 flux for each day of the year and we then calculate the deviation from this mean for each daily observation between 2000 and 2012. This ensures that we keep the same number of observations and remove most of the effects of changes in the length of the day. We calculate the same deviation from the day-of-year mean for the cloud properties for consistency. The same deviations are calculated for the 2000–05 ground-based data. In the rest of this paper, we will occasionally refer to these quantities as anomalies.

Whether we examine ground or satellite observations, as a first-order approximation we assume a linear relationship between the flux and the cloud cover anomalies (as suggested by scatterplots). Therefore, we use a simple least squares regression method to extract the slope and the coefficient of determination R^2. The slope represents the sensitivity of downward shortwave–longwave fluxes to a change in cloud property, and the R^2 value informs us as to the strength of the relationship between the two variables. By using the anomalies as explained above, we not only remove the seasonal trend, we also ensure that the assumption of independence of the variables in the regression is met.

The beginning of our study period includes two years with only *Terra* data. We tested the impact of these two years by conducting our study with data from 2002 onward and found no differences in our conclusions.

Consequently, we decided to keep these first two years to ensure a greater sample size.

c. *Comparison between ground-based and satellite datasets*

Table 1 shows a comparison of the ground-based and satellite-derived measurements of cloud cover and surface shortwave flux at the 11 stations shown in Fig. 1. The differences in surface flux between the ground-based and CERES data are large, with a negative bias ranging between -67 and $-41\,\mathrm{W\,m^{-2}}$ depending on the station (approximately 20%). However, the standard deviations are relatively small and the R^2 coefficient is large, with values between 0.7 and 0.9. Kato et al. (2012), among others (e.g., Hakuba et al. 2013), discussed the impact of spatial resolution in an environment with variable topography and found uncertainties close to the standard deviations found here at two high-elevation sites in the Rockies and the Alps. However, their biases were positive and much smaller. Philipona (2002 and references therein) described issues with ground observations of shortwave flux that may not be taken into account at the stations used herein and, if uncorrected, would underestimate surface fluxes. For both CERES and the ground instruments, it is possible that distinct changes in the instrument sensitivity over time will affect the value of the daily shortwave downward flux. However, we find that over such a short period of time, the trend is small (e.g., Wang 2014), so changes in the difference between CERES and the ground-based flux are small. Finally, it is also possible that CERES fluxes are systematically larger than the ground-based observations because the spectral range of the ground-based pyranometer (0.3–3 μm; http://www.rm17.com/product_227274.html) is smaller than CERES (0.3–5 μm). Since both products have very similar seasonalities, when we compare the deviation from the day-of-year mean of the surface flux between the ground-based and CERES data, the bias becomes negligible between -0.4 and $0.2\,\mathrm{W\,m^{-2}}$ (less than 1% bias). Our study explores the sensitivities; therefore, the bias in the anomalies of the flux affects our conclusions more than the bias in the absolute values of the surface flux.

The cloud cover bias between daily ground-based and MODIS data is fairly small, but the standard deviations are relatively large and R^2 is smaller than that found in the shortwave flux comparison (Table 1). When we plot the difference between MODIS and ground-based cloud cover as a function of ground-based cloud cover, we find that the bias is slightly positive for small values of the ground-based cloud cover and negative for large values of the ground-based cloud cover (not shown). Consequently, if we calculate the difference in cloud cover between two distinct instants in our time series, the absolute value of the MODIS change in cloud cover will be smaller than the ground-based change. However, as for the shortwave flux, when we compare cloud cover as deviations from the day-of-year mean, the bias is reduced to less than 1%, albeit with similar standard deviation and R^2 values.

3. The impact of cloud cover on surface fluxes at the ground stations

Since we found similar differences between ground-based and satellite products at all stations, we arbitrarily chose the Lhasa station to simplify our discussion of the ground-based relationship between cloud cover and shortwave flux. This station sits at 3649 m and is located in the southeastern part of the Tibetan Plateau at 29.67°N, 91.14°E. However, we performed the same study at all stations, and the main results are included in the discussion below.

Using the ground-based observations of the total cloud cover at Lhasa, we explore how clouds impact the downward shortwave flux for each season. Figure 2 shows the seasonal relationship between the flux and cloud cover anomalies at Lhasa. For all seasons, as explained in the previous section, we assume a linear relationship between the flux and cloud cover anomalies, so we perform a least squares regression. We indicate in each panel of Fig. 2 the slope and the R^2 coefficient. The slopes, or sensitivities of surface downward shortwave flux to changes in cloud cover, are also given in Table 2, for Lhasa and the other 10 stations.

The sensitivities change with seasons. The absolute value of the winter sensitivity of downward shortwave flux to changes in cloud cover is about half that found in summer at Lhasa. The magnitude of the autumn sensitivity is only slightly larger than that in winter, whereas in spring the sensitivity is slightly lower in magnitude than it is in summer. Although the absolute values of the sensitivities can differ between the stations, the seasonal variations are similar. The approximation of a linear relationship for the ground-based data (Figs. 2a–d) does not appear to be the best fit, as the R^2 is fairly low in all seasons; that is, less than 50% of the variance in shortwave flux is explained by the cloud cover changes. This is true for most stations, although we find some slight variations in R^2 (Table 2). One issue mentioned in the previous section was that the ground-based cloud cover includes nighttime observations. As a consequence, the cloud cover anomalies may not correspond well to the daytime surface flux anomalies.

We next examine the same relationship but this time using MODIS and CERES deviations from the day-of-year

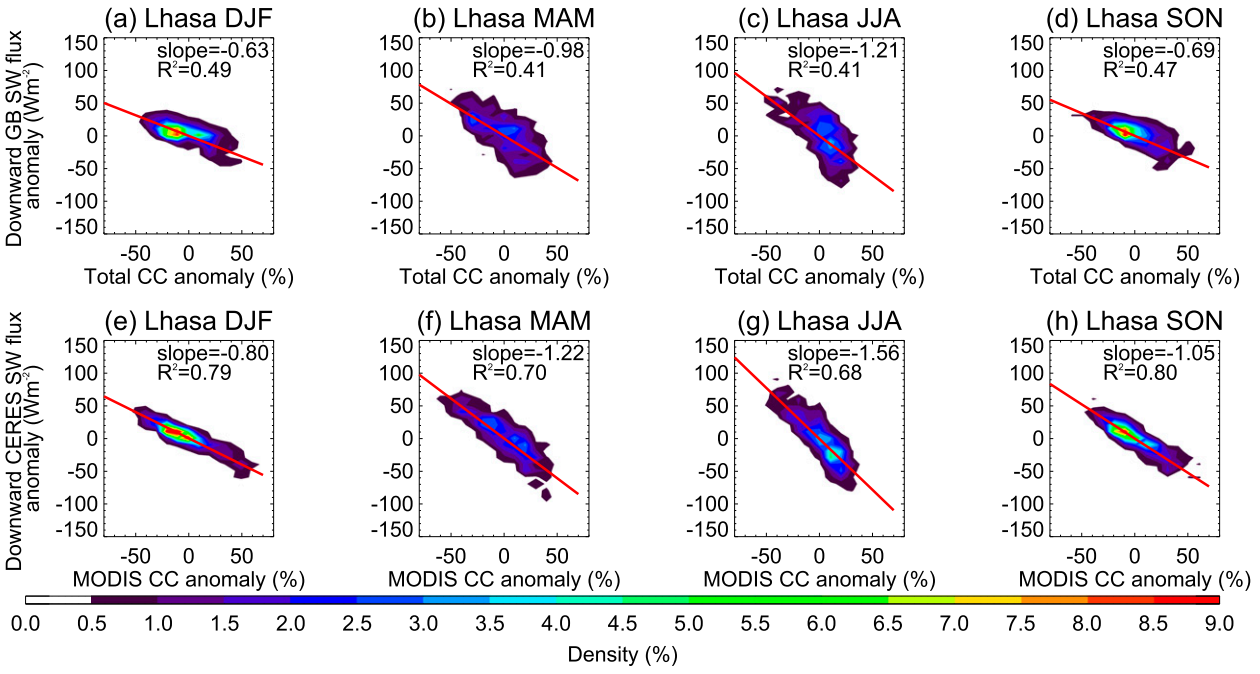

FIG. 2. Deviation from the day-of-year mean in downward shortwave (SW) flux vs deviation in CC at Lhasa by season [winter, December–February (DJF); spring, March–May (MAM); summer, June–August (JJA); autumn, September–November (SON)], using (a)–(d) ground-based and (e)–(h) satellite observations (CERES and MODIS). The slope and R^2 are obtained using linear regression (see also Table 2). The red lines show the linear fit. The color bar indicates the density of data points that fall into a 10% CC and 10 W m^{-2} SW flux anomaly range.

mean for the 1° × 1° grid cell that includes Lhasa (Figs. 2e–h). The linear fit is a much better approximation of the relationship between the flux and cloud cover anomalies when using these datasets at Lhasa. This is also true for most stations, although there are some exceptions, such as Ganzhi in winter where the ground-based observations yield a larger R^2 than the satellite data (Table 2). For all seasons, the R^2 coefficient is greater than 0.5 at Lhasa (Table 2). Although the seasonal variations of the ground-based and satellite observations are similar, the satellite sensitivities are larger and a better fit for most seasons and stations (Table 2). As explained in the previous section, increases in cloud cover detected by MODIS may be underestimated compared to ground-based observations. Because shortwave fluxes do not have this issue, we would expect the slope of the regression to be larger with the satellite data than ground-based data. This is consistent with what we find (Table 2). It is unclear whether the sensitivities obtained from the ground stations are more realistic. There are known issues with MODIS cloud cover (Ackerman et al. 2008), but as discussed in the previous section, the ground-based sensitivities may be inaccurate since the daily ground-based cloud cover includes both day and night observations when the fluxes are obviously only for daytime. To test how this would affect the linear regression, we use MODIS daily (day + night) averages at Lhasa and perform a linear regression against shortwave flux anomalies. The change in R^2 between using daytime-only and daytime and nighttime cloud cover is given in Table 2 (third row). It reveals that indeed diurnal changes in cloud cover cause the daily means to be less well correlated with the shortwave flux anomalies than the day-only means. Consequently, we suggest that a linear regression would give better results with the ground-based data if we could use daytime-only cloud cover.

The average sensitivity of surface shortwave flux to changes in cloud cover over all stations is similar between the ground-based and satellite observations in winter at $-0.5 \pm 0.1\,\mathrm{W\,m^{-2}\,\%^{-1}}$. In summer it reaches -1.5 ± 0.3 and $-1.8 \pm 0.2\,\mathrm{W\,m^{-2}\,\%^{-1}}$ according to ground-based and satellite observations, respectively. As opposed to the ground observations, the MODIS data provide complete spatial coverage and additional information on cloud optical thickness. Hence, we use the satellite-based dataset to explore the impact of clouds on the surface shortwave flux over the entire plateau region, bearing in mind that the satellite-derived sensitivities may be overestimated.

Figure 2 and Table 2 highlight two interesting points: there are 1) seasonal changes in sensitivity and 2) a slight deviation of the sensitivities from the linear fit. Both

TABLE 2. Seasonal sensitivities ($W\,m^{-2}\,\%^{-1}$) of surface downward SW flux to changes in CC at 11 stations as obtained from the ground-based and satellite (CERES and MODIS) instruments. The coefficient of determination is given in parentheses. The CC is a day and night daily average for the ground-based measurements and daytime only for the satellite data. At Lhasa, one row is added to include sensitivities for both day and night CC averages.

Station	Product	DJF	MAM	JJA	SON
Lhasa	GB	−0.63 (0.49)	−0.98 (0.41)	−1.21 (0.41)	−0.69 (0.47)
	Satellite (daytime)	−0.80 (0.79)	−1.22 (0.70)	−1.56 (0.68)	−1.05 (0.80)
	Satellite (day and night)	−0.97 (0.62)	−1.23 (0.50)	−1.40 (0.62)	−1.04 (0.68)
Gangcha	GB	−0.39 (0.39)	−1.05 (0.43)	−1.60 (0.55)	−0.83 (0.49)
	Satellite (daytime)	−0.40 (0.38)	−1.22 (0.59)	−1.91 (0.80)	−1.01 (0.67)
Ge'ermu	GB	−0.38 (0.45)	−0.88 (0.39)	−1.22 (0.52)	−0.63 (0.44)
	Satellite (daytime)	−0.48 (0.45)	−1.04 (0.62)	−1.56 (0.80)	−0.84 (0.69)
Xining	GB	−0.44 (0.50)	−1.06 (0.43)	−1.62 (0.58)	−0.83 (0.48)
	Satellite (daytime)	−0.49 (0.52)	−1.41 (0.66)	−1.97 (0.78)	−1.19 (0.70)
Ge'er	GB	−0.70 (0.44)	−1.17 (0.62)	−1.18 (0.60)	−0.82 (0.51)
	Satellite (daytime)	−0.73 (0.55)	−0.92 (0.69)	−1.44 (0.76)	−0.99 (0.81)
Naqu	GB	−0.74 (0.48)	−1.16 (0.42)	−1.71 (0.53)	−0.89 (0.48)
	Satellite (daytime)	−0.61 (0.62)	−0.95 (0.50)	−1.75 (0.75)	−0.98 (0.67)
Yushu	GB	−0.32 (0.38)	−0.91 (0.36)	−1.25 (0.60)	−0.64 (0.45)
	Satellite (daytime)	−0.49 (0.50)	−0.94 (0.44)	−1.85 (0.79)	−1.03 (0.67)
Guoluo	GB	−0.55 (0.45)	−1.11 (0.38)	−1.87 (0.63)	−0.89 (0.48)
	Satellite (daytime)	−0.50 (0.53)	−1.15 (0.51)	−1.98 (0.80)	−1.08 (0.69)
Changdu	GB	−0.72 (0.57)	−1.09 (0.37)	−1.40 (0.50)	−0.80 (0.48)
	Satellite (daytime)	−0.55 (0.67)	−0.95 (0.51)	−1.90 (0.74)	−1.02 (0.69)
Ganzhi	GB	−0.51 (0.51)	−1.04 (0.38)	−1.30 (0.48)	−0.83 (0.49)
	Satellite (daytime)	−0.39 (0.46)	−0.74 (0.38)	−1.87 (0.79)	−1.07 (0.67)
Hongyuan	GB	−0.73 (0.46)	−1.65 (0.44)	−1.98 (0.55)	−1.26 (0.56)
	Satellite (daytime)	−0.43 (0.46)	−0.96 (0.46)	−1.90 (0.80)	−1.12 (0.70)

suggest that other factors influence the surface downward shortwave flux. The residual signal can be caused by a number of factors, including the following:

1) Measurements of flux and cloud may change over time as a result of changes in instrument sensitivity or in retrieval techniques. However, when we checked how the bias between the CERES and ground-based fluxes changed over the 2000–05 period, we did not find a significant trend.
2) Changes in surface albedo will affect the diffuse component of the surface flux (e.g., Pinty et al. 2005). To estimate the magnitude of this effect is intricate and goes beyond the scope of the present study.
3) Changes in snow cover will affect both factors 1 and 2 above. Based on the work of Pu and Xu (2009) and our own examination of the MODIS monthly snow cover retrievals (Hall et al. 2002, 2006), we find that, at least over the central part of the plateau, snow cover is low, in part owing to the shadowing effect of the high mountains to the south and west. Ackerman et al. (2008) report that at night cloud detection over bright surfaces is difficult. Here, we use daytime cloud cover, and as there is little snow, we did not find any correlation between differences in MODIS–ground-based cloud cover and snow cover. Consequently, we assume that changes in snow cover will have a very small impact on our results.
4) Aerosols will undeniably have an impact on the changes in surface downward shortwave flux. You et al. (2013) find that the decrease in clear-sky flux over the past 50 decades over the Tibetan Plateau could only be explained by a steady increase in the 550-nm aerosol optical thickness. However, Haywood et al. (2011) find that globally an increase in water vapor can overwhelm the effect of aerosols on surface fluxes in clear-sky conditions, and also Yang et al. (2012) argue that changes in aerosol over the Tibetan Plateau are less important than changes in cloud optical thickness for explaining trends there. Liepert (2002) also found that both changes in cloud cover and optical thickness have a significant impact on surface radiation changes over the United States.

Thus, we next explore the impact of concomitant changes in cloud cover and optical thickness on surface fluxes using satellite observations over the entire Tibetan Plateau. Because of the large contrast in sensitivities between winter and summer, we focus on these two seasons.

4. Sensitivity of surface downward fluxes to changes in cloud properties over the Tibetan Plateau

We average MODIS cloud cover and optical thickness separately for all 13 winters and summers between 2000 and 2012 for the entire Tibetan Plateau region. Figure 3a shows that during winter, the southern portion of the plateau has very low cloud cover, in contrast with the northern band where cloud cover can exceed 85%. This reverses in summer, with large cloud cover to the south and a smaller amount to the north (Fig. 3b). The seasonal cycle in cloud cover differs distinctly between the north and south, and suggests the greater influence of the midlatitude westerlies in the north, and of the south Asian monsoon in the south. A strong seasonal cycle is also found when comparing the winter and summer averages of cloud optical thickness (Figs. 3c and 3d, respectively). In winter, clouds over the plateau are optically thin, with a region of relatively thicker clouds along the Himalayas and other areas of steep altitude gradients (Fig. 3c). In contrast, summer clouds are much thicker and, apart from the extreme northwestern and southwestern corners, much more uniform (Fig. 3d).

a. *Sensitivity of surface downward shortwave flux to changes in cloud properties*

For each grid cell where we have MODIS and CERES data, we performed a multiple regression of the surface shortwave flux anomalies with respect to both cloud cover and cloud optical thickness anomalies. We ensured that these two cloud parameters are weakly correlated ($R \approx 0.22$). The regression solves for the coefficients in the following relation:

$$F_{\mathrm{SW}}^{\downarrow} \approx \mathrm{const} + \alpha_{\mathrm{CC}} \times \mathrm{CC} + \alpha_{\tau} \times \tau, \qquad (1)$$

where the coefficients α_{CC} and α_{τ} represent the sensitivities of the flux to cloud cover (CC) and optical thickness (τ), respectively (Figs. 3e–h).

In winter, the cloud cover has a relatively small impact on the flux (in absolute value), of less than 1 W m^{-2} for a 1% change (Fig. 3e), but in summer (Fig. 3f) there is a northwest–southeast progression of sensitivities with a relatively smaller impact of cloud cover to the northwest than to the southeast.

In winter, the sensitivity to optical thickness is small in the region of large optical thickness and low cloud cover along the Himalayas and relatively larger in the central part of the plateau (Fig. 3g). In summer (Fig. 3h), sensitivities to optical thickness are much larger, with a maximum to the south of the Himalayas, and relatively lower sensitivities in the central plateau.

Figures 3i,j show that when considering only the cloud cover anomalies, the R^2 of the regression between the shortwave flux and the cloud cover is greater than 0.5 in the southern half of the plateau in winter and everywhere in summer, except for a region to the south of the Himalayas where cloud cover is large (Fig. 3b) and the sensitivity of the flux to optical thickness anomalies is largest (Fig. 3h). When the regression includes both cloud cover and optical thickness anomalies [Eq. (1)], the coefficient of determination of the multiple regression increases, and exceeds 0.5 over a larger area than when regressing against cloud cover alone, including more of the northern part of the plateau in winter (Fig. 3k) and the entire region in summer (Fig. 3l), in particular the region south of the Himalayas. Therefore, in both seasons, although cloud cover anomalies alone explain a significant portion of the variance, adding the optical thickness anomalies into the regressions improves the overall R^2 by ~15%.

Returning to the impact of aerosols on the surface downward shortwave flux, we collected concurrent daily MODIS 550-nm aerosol optical thickness retrievals (Remer et al. 2005). There is no correlation between the aerosol and cloud optical thickness retrievals ($R \sim 0.04$), so we perform a multiple regression of the surface shortwave flux against cloud cover, cloud optical thickness, and aerosol optical thickness. We find that the R^2 of the regression is either identical to or less than the R^2 obtained when regressing against cloud cover and optical thickness (not shown). There are obvious problems with this approach: one being that the aerosol optical thickness is only retrieved when clouds are absent. So one needs to assume that the optical thickness at the time of the aerosol retrievals is representative of the daily mean. Also, there are many missing daily retrievals in the aerosol record, especially in summer when cloud cover is large. In addition, the direct aerosol effect is weak when clouds are present and only of real importance when the cloud cover is null. Finally, the datasets at our disposal do not allow for any analysis of the indirect effect of aerosols on the cloud properties. All these issues hinder any possible improvements in the linear fit when adding the contribution of the aerosol optical thickness to the regression.

To better understand how cloud cover and optical thickness anomalies impact the shortwave flux, we bin the changes in shortwave flux according to coincident increments of changes in cloud cover and in cloud optical thickness, that is, increases or decreases in 5% and 5-unit increments respectively. We then calculate the average change in shortwave flux in both space and time in each 5% or 5-unit bin (Fig. 4). As expected, the flux increases (decreases) when both cloud cover and optical thickness decrease (increase). However, Fig. 4 indicates that for

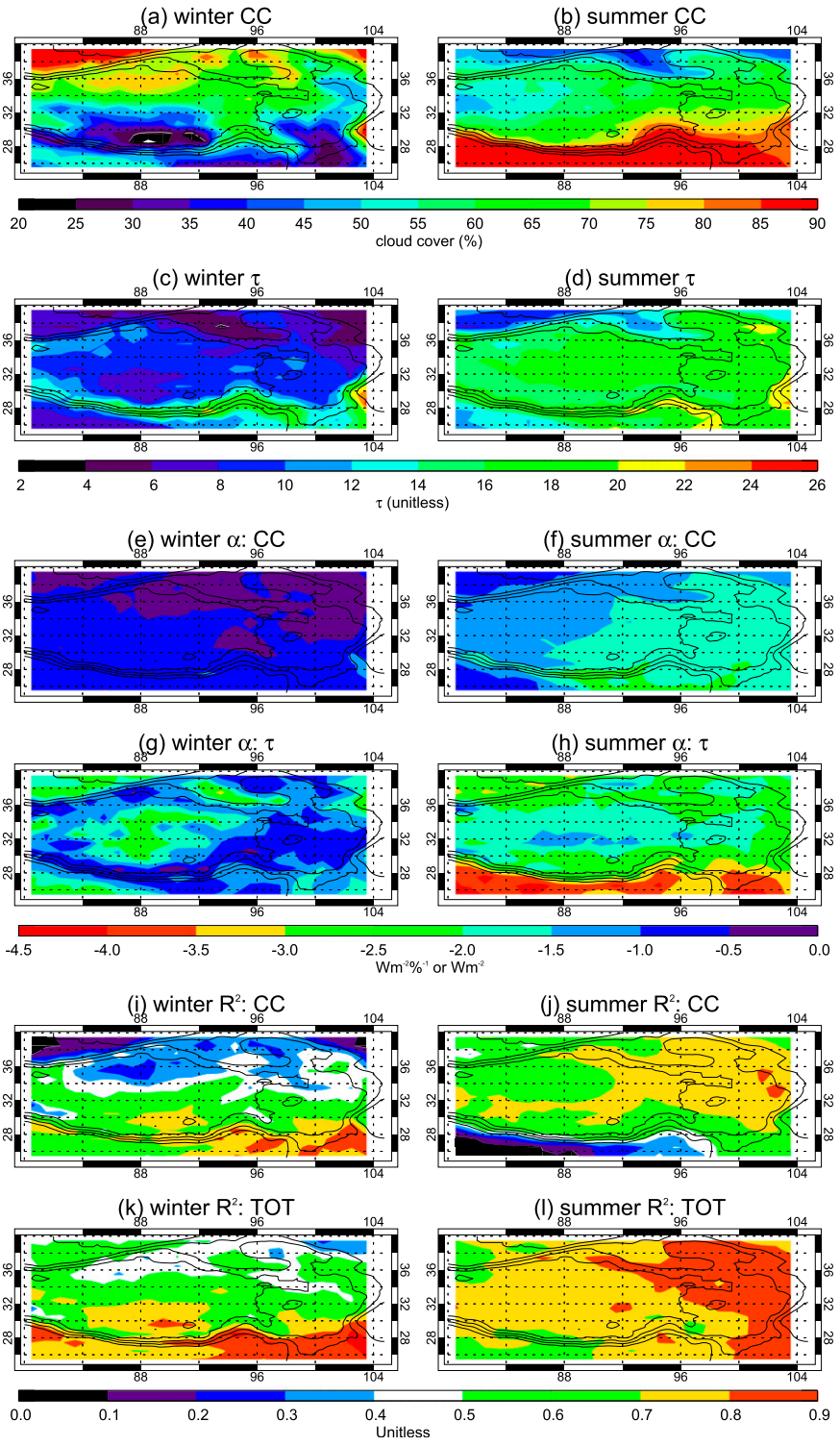

FIG. 3. Average for 2000–12 of MODIS for (left) winter and (right) summer: (a),(b) CC and (c),(d) τ; slopes α of multiple regression [cf. Eq. (1)] of shortwave flux anomalies on (e),(f) CC and (g),(h) τ; R^2 with respect to (i),(j) CC alone and (k),(l) both CC and τ (TOT). Here and in subsequent figures, the black contours indicate the topography.

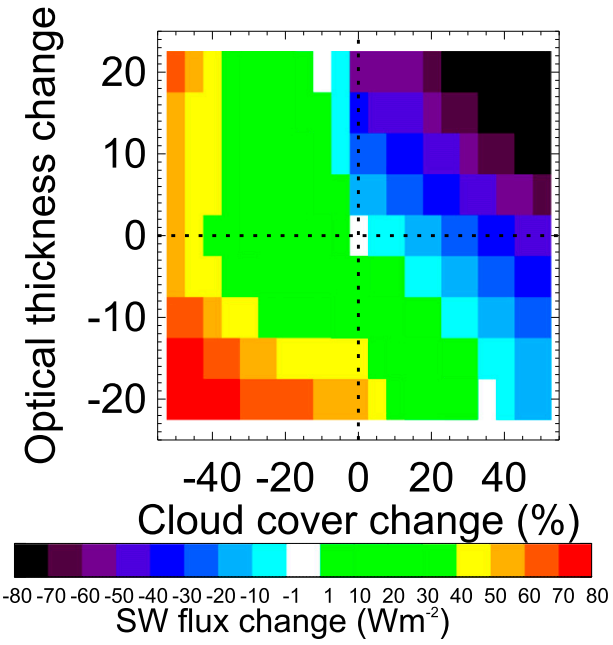

FIG. 4. The average in time and space of the change in surface downward SW flux as a function of changes in cloud optical thickness and cloud cover for the entire Tibetan Plateau region between 2000 and 2012.

a small decrease in cloud cover (less than 5% in absolute value), accompanied by an increase in optical thickness, the shortwave flux can decrease, as found by Yang et al. (2012). The inverse is also true, namely that the flux can increase when cloud cover increases are accompanied by a decrease in optical thickness. This highlights the importance of accounting for changes in optical thickness when exploring changes in surface downward solar flux.

Overall, we find that on the plateau the sensitivity of the downward shortwave flux to changes in cloud cover varies between winter and summer (Figs. 3e,f). In addition, for each season the sensitivities change with location as well, and this may depend on the local climatology of cloud cover and optical thickness. In fact, Fig. 5a shows that the sensitivity depends little on cloud cover and optical thickness in winter when both cloud cover and optical thickness are small, although for optical thicknesses between 4 and 12, we note a slight increase in sensitivity as cloud cover increases. Similarly in summer, there is little correlation between the sensitivities and cloud cover for optical thicknesses less than about 12 (Fig. 5a). However, for larger opacities, sensitivities (in absolute values) increase with increasing cloud cover. So the sensitivity of changes in shortwave flux to changes in cloud cover is nearly independent of cloud cover in winter, although Fig. 5b suggests a slight dependence on cloud optical thickness. In contrast, summer sensitivities clearly depend on optical thickness (Fig. 5b) and on cloud cover when cloud opacity exceeds 12 (Fig. 5a).

b. *Sensitivity of surface downward longwave flux to changes in cloud properties*

To complete our analysis of the impact of changes in cloud cover and optical thickness on surface radiation, we

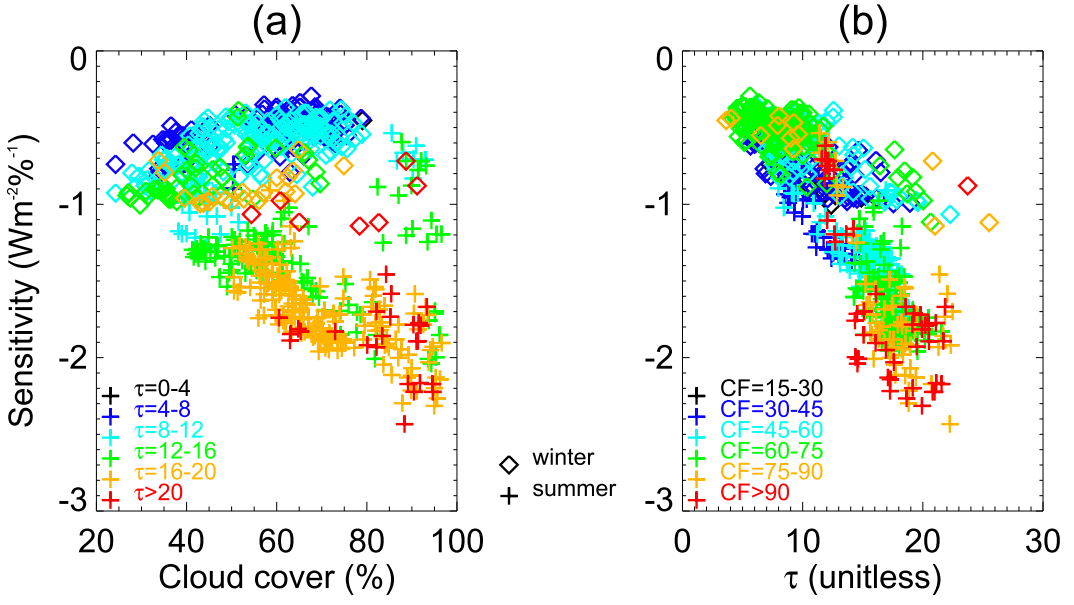

FIG. 5. Sensitivity of CERES downward SW flux to MODIS CC for the entire Tibetan Plateau region for 2000–12 during winter (diamonds) and summer (plus signs) as a function of (a) MODIS cloud cover with seasonal mean τ indicated in color from the 0–4 range (black) to >20 (red) and of (b) MODIS cloud optical thickness with seasonal mean CC indicated in color from the 15%–30% range (black) to >90% (red).

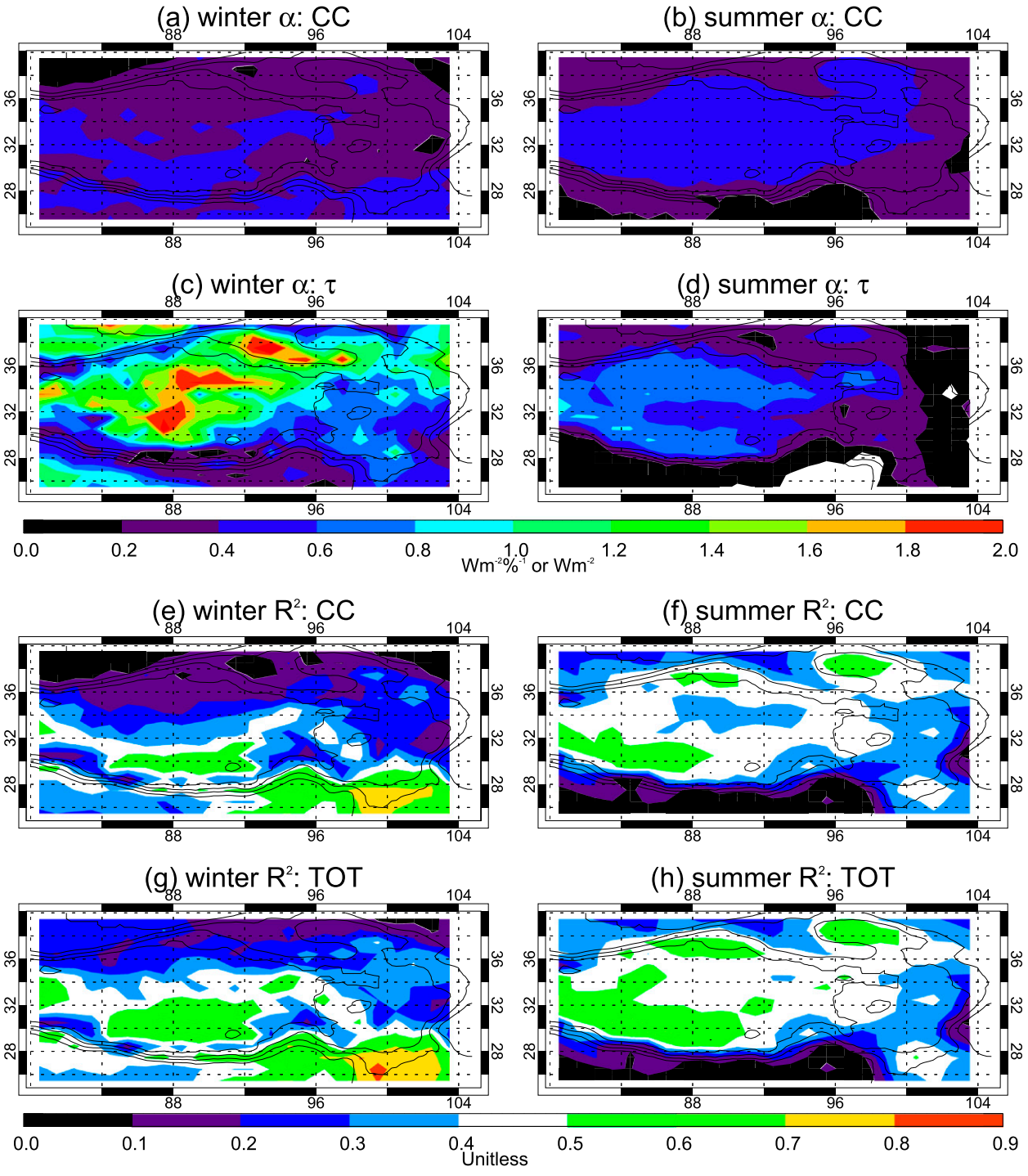

FIG. 6. For (left) winter and (right) summer, slope α of multiple regression of deviation of the day-of-year mean in CERES surface downward longwave flux on MODIS (a),(b) CC and (c),(d) τ and R^2 for (e),(f) CC alone and (g),(h) both CC and τ (TOT).

examine their daytime impact on surface downward longwave flux. Again, we perform a (multiple) regression on the cloud cover alone and then together with optical thickness and examine the corresponding sensitivities and R^2 (Fig. 6).

In winter, changes in cloud cover have a relatively small impact on the longwave flux (Fig. 6a) as compared with their impact on the shortwave flux (Fig. 3e), albeit with a slightly larger impact to the south. In contrast,

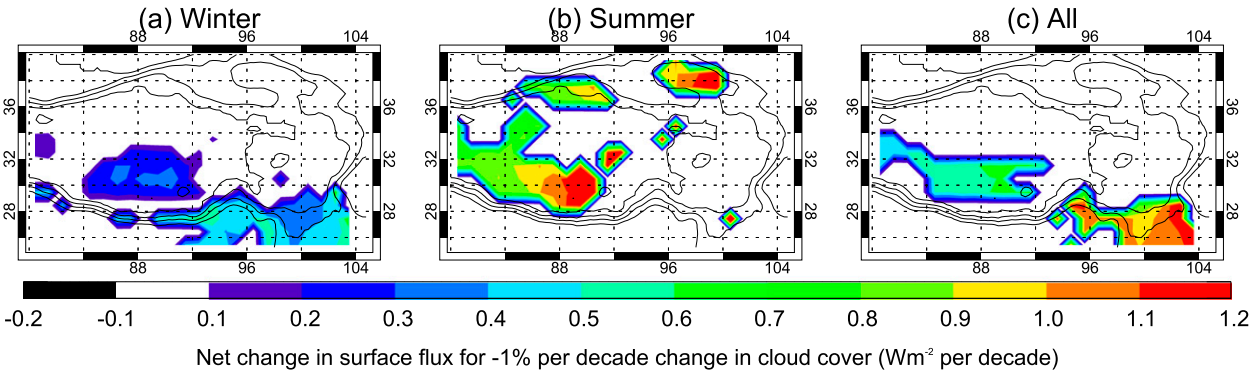

FIG. 7. Maps of change in net daytime surface flux (sum of longwave and shortwave) for a −1% change in CC per decade during (a) winter, (b) summer, and (c) all seasons. Areas where the R^2 of the multiple regressions on CC and optical thickness is < 0.5 are in white.

a change in optical thickness has a larger impact on the longwave flux in the central part of the plateau than to the south (Fig. 6c).

In summer, the sensitivity to cloud cover changes is larger in the central part of the plateau than in the outer regions (Fig. 6b). The sensitivity to changes in optical thickness is also slightly larger over the central plateau (Fig. 6d) but both cloud cover and optical thickness have a smaller impact on the longwave flux than the shortwave flux in summer.

When considering the impact of cloud cover alone, the R^2 coefficient is small for both winter and summer (Figs. 6e,f). This is expected as the surface longwave flux depends strongly on water vapor amount and temperature (e.g., Rangwala et al. 2009) and, more specifically for clouds, the temperature at cloud base. Information on cloud-base temperature is not available from either satellites or ground stations. There is some improvement when both cloud cover and optical thickness are included in the regression (Figs. 6g,h). In winter, these two variables seem to be more influential in the southeast corner and across the south-central part of the plateau (Fig. 6h). In summer, only this latter region has R^2 values above the 0.5 threshold (Fig. 6h).

c. Discussion

Duan and Wu (2006) reported a decrease in daytime cloud cover of about 1% decade^{-1} during the last three decades over the Tibetan Plateau. This trend was found as an average over stations mostly in the eastern half of our study region (east of 85°E; Fig. 1). In the following, assuming that the trend is similar in the western half of our study region, we use the sensitivities derived above to estimate the impact of a 1% decrease per decade in cloud cover on the daytime surface downward net flux (the sum of longwave and shortwave fluxes). Here, we explore the impact of clouds only where the R^2 of the regressions is above 0.5. Figure 7a shows that, in winter, a decrease in cloud cover of 1% decade^{-1} causes an increase in downward net fluxes of 0.2–0.4 W m^{-2} decade^{-1} (between −1 and −0.5 W m^{-2} decade^{-1} for shortwave flux and 0.6–0.8 W m^{-2} decade^{-1} for longwave flux) in the south-central plateau region. The impact is slightly larger farther to the southeast. In summer, the impact is largest over the central part of the plateau, with changes in net fluxes up to 1.2 W m^{-2} decade^{-1} (Fig. 7b). For all seasons combined, the impact is about 0.5–0.6 W m^{-2} decade^{-1} in the south-central part of the plateau and 1.0–1.2 W m^{-2} decade^{-1} in the southeastern corner (Fig. 7c). The net flux for all seasons combined differs from the summer net flux because the addition of winter and intermediate seasons affects both the magnitude of the net flux and the value of R^2. The cloud effects on the net flux are of the same order as the impact of the measured changes in specific humidity on surface longwave fluxes over the Tibetan Plateau for the same period (Rangwala et al. 2009).

Considering only the solar flux, and focusing on Lhasa, ground-based and satellite observations agree that for a decrease in cloud cover of 1% decade^{-1}, with other variables kept fixed, Lhasa should experience an increase in shortwave flux of about 1.2–1.5 W m^{-2} in summer (about 6%) and about half that in winter (0.6–0.8 W m^{-2}, about 4%).

Since we have not found any studies of trends in optical thickness for this region, we calculate how much the optical thickness would have to increase to completely cancel out the impact of the 1% decrease in cloud cover. Still using only solar flux, and focusing on the central region of the plateau (a 6° radius zone centered on 32°N, 88°E), we calculate the impact of a decrease in cloud cover of 1% decade^{-1} accompanied by an increase in optical thickness. In winter, cloud optical thickness has to increase by 0.5 decade^{-1} (~10% for the entire period) to

cancel the impact of the reduced cloud cover on solar flux. In summer, cloud optical thickness has to increase by about one unit per decade (~5%) to counteract the impact of a 1% decade^{-1} decrease in cloud cover.

At night, MODIS optical thickness retrievals are not available (the algorithm relies on visible channels), and we would also need cloud-base temperatures to get better estimates of how changes in cloud cover impact the downward longwave flux. Trends reported by Duan and Wu (2006) for nighttime cloud cover are positive, and they find that the impact of cloud cover changes on longwave flux at night is greater than the impact of cloud cover changes on both shortwave and longwave fluxes during the day. However, our daytime results suggest that cloud cover information alone is not sufficient to predict the impact of cloud changes on surface fluxes, and ultimately temperature, because during the day changes in optical thickness can offset or enhance the impact of clouds on the shortwave flux.

5. Conclusions

In this study, we use satellite estimates of surface downward shortwave flux, as well as retrievals of cloud cover and optical thickness over the Tibetan Plateau, to examine the impact of changes in cloud properties on surface downward shortwave radiation. When comparing cloud cover and surface shortwave flux derived from satellites to ground-based measurements at 11 stations, we find that despite differences between the two sets of measurements and their limitations (e.g., Yang et al. 2008; Kato et al. 2012), daily anomalies in flux and cloud cover are very similar when the seasonal cycle is removed. Both ground-based and satellite measurements indicate that the sensitivity of the surface downward shortwave flux to changes in cloud cover varies with season and does not follow a perfectly linear relationship. The latter could be caused partly by the additional influence of cloud optical thickness on flux. We therefore use satellite retrievals for the entire region to explore and quantify the combined effects of changes in cloud cover and optical thickness on downward shortwave radiation.

We find strong seasonal and regional variations in cloud cover and optical thickness, with larger values in summer than winter. In winter, cloud cover increases with latitude, but in summer the opposite is true. This in turn affects the sensitivity of the surface downward shortwave flux to changes in cloud cover. Over the entire region, clouds are optically thicker in summer than winter, except possibly along the regions of steep altitude gradients where the variations in optical thickness are more modest. Large-scale weather patterns may contribute to these different seasonal and regional cloud characteristics, possibly modulated by global oscillations, such as the North Atlantic Oscillation or Arctic Oscillation in winter (e.g., Cuo et al. 2013). In summer the South and East Asian monsoons trigger moist convection, and their impact decreases with increasing latitude [see Cuo et al. (2013) for a detailed analysis]. At higher latitudes, gradual heating of the plateau favors local convection and an increase in precipitation (Yang et al. 2014).

Overall, we find that changes in surface shortwave flux are predominantly affected by changes in cloud cover. However, we also find that changes in optical thickness are not negligible and, in some cases, can actually offset or enhance the impact of cloud cover changes on the surface shortwave flux. In fact, we find that, over the entire region, the sensitivity of the shortwave flux to changes in cloud cover depends on the actual cloud optical thickness in both winter and summer, but it depends on the actual cloud cover only in summer and when cloud optical thicknesses are greater than 12. The shortwave flux decreases as both cloud cover and optical thickness increase, but the shortwave flux can decrease when decreases in cloud cover are accompanied by a sufficiently large increase in optical thickness.

The impact of a change in cloud cover and optical thickness on the daytime surface downward longwave flux also reveals that changes in optical thickness are important at these wavelengths, in particular during the winter when the atmosphere is the coldest and driest (i.e., when the impact of water vapor is smallest). We calculate the impact of a change in cloud cover on the surface downward net fluxes. Duan and Wu (2006) report a decrease in daytime cloud cover of 1% decade^{-1} over the last three decades, for stations located in the eastern half of our study region. Based on our calculations, assuming this trend to be similar over our entire region of interest, we find that this 1% decrease in cloud cover would cause a modest increase in downward shortwave flux over the central region of the plateau, and to the southeast in winter, with a much more significant increase in summer over the central part of the plateau. If this decrease in cloud cover were accompanied by an increase in cloud optical thickness, as suggested by Yang et al. (2012), a 0.5 increase would counteract the impact of the cloud cover change in winter and reduce this impact by half in summer. Consequently, trends in cloud cover alone may not be sufficient to predict changes in surface downward radiation and, ultimately, changes in surface temperatures.

Acknowledgments. The ground-based climate data were obtained from the China Meteorological Administration.

We thank Eric Sinsky for the quality control of the data and reformatting of the files and Yonghua Chen for translating the technical specifications of the Chinese pyranometers DYF-4. The CERES data were obtained from the Atmospheric Science Data Center at the NASA Langley Research Center. The MODIS daily cloud and aerosol files were obtained from the Goddard Space Flight Center level 1 and Atmosphere Archive and Distribution System. The MODIS monthly snow products were obtained from the National Snow and Ice Data Center. The GTOPO30 digital elevation model data were obtained at the U.S. Geological Survey website (https://lta.cr.usgs.gov/GTOPO30). This work was funded by the National Science Foundation (Grants 1064281 and 1064326). JRM received support from the New Jersey Agricultural Experiment Station and the USDA–National Institute for Food and Agriculture, Hatch Project NJ32103. The authors thank Mark Miller and three anonymous reviewers for their very helpful comments.

REFERENCES

Ackerman, S. A., R. E. Holz, R. Frey, E. W. Eloranta, B. C. Maddux, and M. McGill, 2008: Cloud detection with MODIS. Part II: Validation. *J. Atmos. Oceanic Technol.,* **25,** 1073–1086, doi:10.1175/2007JTECHA1053.1.

Cuo, L., Y. Zhang, Q. Wang, L. Zhang, B. Zhou, Z. Hao, and F. Su, 2013: Climate change on the northern Tibetan Plateau during 1957–2009: Spatial patterns and possible mechanisms. *J. Climate,* **26,** 85–109, doi:10.1175/JCLI-D-11-00738.1.

Doelling, D. R., and Coauthors, 2013: Geostationary enhanced temporal interpolation for CERES flux products. *J. Atmos. Oceanic Technol.,* **30,** 1072–1090, doi:10.1175/JTECH-D-12-00136.1.

Duan, A., and G. Wu, 2006: Change of cloud amount and the climate warming on the Tibetan Plateau. *Geophys. Res. Lett.,* **33,** L22704, doi:10.1029/2006GL027946.

Hakuba, M. Z., D. Folini, A. Sanchez-Lorenzo, and M. Wild, 2013: Spatial representativeness of ground-based solar radiation measurements. *J. Geophys. Res.,* **118,** 8585–8597, doi:10.1002/jgrd.50673.

Hall, D. K., G. A. Riggs, V. V. Salomonson, N. E. DiGirolamo, and K. J. Bayr, 2002: MODIS snow-cover products. *Remote Sens. Environ.,* **83,** 181–194, doi:10.1016/S0034-4257(02)00095-0.

——, V. V. Salomonson, and G. A. Riggs, 2006: MODIS/*Terra* snow-cover monthly L3 global 0.05Deg CMG, version 5: 2000–2005. National Snow and Ice Data Center, Boulder, CO. [Available online at http://tinyurl.com/qyd53nv.]

Haywood, J. M., N. Bellouin, A. Jones, O. Boucher, M. Wild, and K. P. Shine, 2011: The roles of aerosol, water vapor and cloud in future global dimming/brightening. *J. Geophys. Res.,* **116,** D20203, doi:10.1029/2011JD016000.

Kaiser, D. P., 1998: Analysis of total cloud amount over China, 1951–1994. *Geophys. Res. Lett.,* **25,** 3599–3602, doi:10.1029/98GL52784.

——, and Y. Qian, 2002: Decreasing trends in sunshine duration over China for 1954–1998: Indication of increased haze pollution? *Geophys. Res. Lett.,* **29,** 2042, doi:10.1029/2002GL016057.

Kato, S., and Coauthors, 2011: Improvements of top-of-atmosphere and surface irradiance computations wth *CALIPSO*-, *CloudSat*-, and MODIS-derived cloud and aerosol properties. *J. Geophys. Res.,* **116,** D19209, doi:10.1029/2011JD016050.

——, N. G. Loeb, D. A. Rutan, F. G. Rose, S. Sun-Mack, W. F. Miller, and Y. Chen, 2012: Uncertainty estimate of surface irradiances computed with MODIS-, *CALIPSO*- and *CloudSat*-derived cloud and aerosol properties. *Surv. Geophys.,* **33,** 395–412, doi:10.1007/s10712-012-9179-x.

——, ——, F. G. Rose, D. R. Doelling, D. A. Rutan, T. E. Caldwell, L. Yu, and R. A. Weller, 2013: Surface irradiances consistent with CERES-derived top-of-atmosphere shortwave and longwave irradiances. *J. Climate,* **26,** 2719–2740, doi:10.1175/JCLI-D-12-00436.1.

Liepert, B. G., 2002: Observed reduction of surface solar radiation at sites in the United States and worldwide from 1961 to 1990. *Geophys. Res. Lett.,* **29,** doi:10.1029/2002GL014910.

Liu, B., M. Xu, M. Henderson, Y. Qi, and Y. Li, 2004: Taking China's temperature: Daily range, warming trends, and regional variations, 1955–2000. *J. Climate,* **17,** 4453–4462, doi:10.1175/3230.1.

Liu, X., and B. Chen, 2000: Climatic warming in the Tibetan Plateau during recent decades. *Int. J. Climatol.,* **20,** 1729–1742, doi:10.1002/1097-0088(20001130)20:14<1729::AID-JOC556>3.0.CO;2-Y.

Minnis, P., 1989: Viewing zenith angle dependence of cloudiness determined from coincident GOES East and GOES West data. *J. Geophys. Res.,* **94,** 2303–2320, doi:10.1029/JD094iD02p02303.

——, and Coauthors, 2011: CERES Edition-2 cloud property retrievals using TRMM VIRS and *Terra* and *Aqua* MODIS data, Part I: Algorithms. *IEEE Trans. Geosci. Remote Sens.,* **49,** 4374–4400, doi:10.1109/TGRS.2011.2144601.

Naud, C. M., and Y.-H. Chen, 2010: Assessment of ISCCP cloudiness over the Tibetan Plateau using *CloudSat-CALIPSO*. *J. Geophys. Res.,* **115,** D10203, doi:10.1029/2009JD013053.

Pepin, N., and J. Lundquist, 2008: Temperature trends at high elevations: Patterns across the globe. *Geophys. Res. Lett.,* **35,** L14701, doi:10.1029/2008GL034026.

Philipona, R., 2002: Underestimation of solar global and diffuse radiation measured at Earth's surface. *J. Geophys. Res.,* **107,** 4654, doi:10.1029/2002JD002396.

Pinty, B., and Coauthors, 2005: Coupling diffuse sky radiation and surface albedo. *J. Atmos. Sci.,* **62,** 2580–2591, doi:10.1175/JAS3479.1.

Platnick, S., M. D. King, S. A. Ackerman, W. P. Menzel, B. A. Baum, J. C. Riédi, and R. A. Frey, 2003: The MODIS cloud products: Algorithms and examples from *Terra*. *IEEE Trans. Geosci. Remote Sens.,* **41,** 459–472, doi:10.1109/TGRS.2002.808301.

Pu, Z., and L. Xu, 2009: MODIS/*Terra* observed snow cover over the Tibet Plateau: distribution, variation and possible connection with the East Asian Summer Monsoon (EASM). *Theor. Appl. Climatol.,* **97,** 265–278, doi:10.1007/s00704-008-0074-9.

Qian, Y., D. P. Kaiser, L. R. Leung, and M. Xu, 2006: More frequent cloud-free sky and less surface solar radiation in China from 1955 to 2000. *Geophys. Res. Lett.,* **33,** L01812, doi:10.1029/2005GL024586.

Rangwala, I., J. R. Miller, and M. Xu, 2009: Warming in the Tibetan Plateau: Possible influences of the changes in surface water vapor. *Geophys. Res. Lett.,* **36,** L06703, doi:10.1029/2009GL037245.

——, E. Sinsky, and J. R. Miller, 2013: Amplified warming projections for high altitude regions of the Northern Hemisphere mid-latitudes from CMIP5 models. *Environ. Res. Lett.,* **8,** 024040, doi:10.1088/1748-9326/8/2/024040.

Remer, L. A., and Coauthors, 2005: The MODIS aerosol algorithm, products, and validation. *J. Atmos. Sci.,* **62,** 947–973, doi:10.1175/JAS3385.1.

Salomonson, V. V., W. L. Barnes, P. W. Maymon, H. E. Montgomery, and H. Ostrow, 1989: MODIS: Advanced facility instrument for studies of the earth as a system. *IEEE Trans. Geosci. Remote Sens.,* **27,** 145–153, doi:10.1109/36.20292.

Shi, G.-Y., T. Hayasaka, A. Ohmura, Z.-H. Chen, B. Wang, J.-Q. Zhao, H.-Z. Che, and L. Xu, 2008: Data quality assessment and the long-term trend of ground solar radiation in China. *J. Appl. Meteor. Climatol.,* **47,** 1006–1016, doi:10.1175/2007JAMC1493.1.

Smith, G. L., K. J. Priestley, N. G. Loeb, B. A. Wielicki, T. P. Charlock, P. Minnis, D. R. Doelling, and D. A. Rutan, 2011: Clouds and Earth Radiant Energy System (CERES), a review: Past, present and future. *Adv. Space Res.,* **48,** 254–263, doi:10.1016/j.asr.2011.03.009.

Wang, B., Q. Bao, B. Hoskins, G. Wu, and Y. Liu, 2008: Tibetan Plateau warming and precipitation changes in East Asia. *Geophys. Res. Lett.,* **35,** L14702, doi:10.1029/2008GL034330.

Wang, K. C., 2014: Measurement biases explain discrepancies between the observed and simulated decadal variability of surface incident solar radiation. *Sci. Rep.,* **4,** 6144, doi:10.1038/srep06144.

Warren, S. G., C. J. Hahn, and J. London, 1985: Simultaneous occurrence of different cloud types. *J. Climate Appl. Meteor.,* **24,** 658–667, doi:10.1175/1520-0450(1985)024<0658:SOODCT>2.0.CO;2.

Wielicki, B. A., B. R. Barkstrom, E. F. Harrison, R. B. Lee, III, G. L. Smith, and J. E. Cooper, 1996: Clouds and the Earth's Radiant Energy System (CERES): An Earth Observing System experiment. *Bull. Amer. Meteor. Soc.,* **77,** 853–868, doi:10.1175/1520-0477(1996)077<0853:CATERE>2.0.CO;2.

Wild, M., 2009: Global dimming and brightening: A review. *J. Geophys. Res.,* **114,** D00D16, doi:10.1029/2008JD011470.

Xia, X., 2010: A closer look at dimming and brightening in China during 1961–2005. *Ann. Geophys.,* **28,** 1121–1132, doi:10.5194/angeo-28-1121-2010.

Yanai, M., C. Li, and Z. Song, 1992: Seasonal heating of the Tibetan Plateau and its effects on the evolution of the Asian summer monsoon. *J. Meteor. Soc. Japan,* **70,** 319–351.

Yang, B., C. Qin, J. Wang, M. He, T. M. Melvin, T. J. Osborn, and K. R. Briffa, 2014: A 3,500-year tree-ring record of annual precipitation on the northeastern Tibetan Plateau. *Proc. Natl. Acad. Sci. USA,* **111,** 2903–2908, doi:10.1073/pnas.1319238111

Yang, K., R. T. Pinker, Y. Ma, T. Koike, M. M. Wonsick, S. J. Cox, Y. Zhang, and P. Stackhouse, 2008: Evaluation of satellite estimates of downward shortwave radiation over the Tibetan Plateau. *J. Geophys. Res.,* **113,** D17204, doi:10.1029/2007JD009736.

——, B. Ding, J. Qin, W. Tang, N. Lu, and C. Lin, 2012: Can aerosol loading explain the solar dimming over the Tibetan Plateau? *Geophys. Res. Lett.,* **39,** L20710, doi:10.1029/2012GL053733.

Ye, D.-Z., and G.-X. Wu, 1998: The role of the heat source of the Tibetan Plateau in the general circulation. *Meteor. Atmos. Phys.,* **67,** 181–198, doi:10.1007/BF01277509.

Ye, J., F. Li, G. Sun, and A. Guo, 2009: Solar dimming and its impact on estimating solar radiation from diurnal temperature range in China, 1961-2007. *Theor. Appl. Climatol.,* **101,** 137–142, doi:10.1007/s00704-009-0213-y.

You, Q., A. Sanchez-Lorenzo, M. Wild, D. Folini, K. Fraedrich, G. Ren, and S. Kang, 2013: Decadal variation of surface solar radiation in the Tibetan Plateau from observations, reanalysis and model simulations. *Climate Dyn.,* **40,** 2073–2086, doi:10.1007/s00382-012-1383-3.

Zhang, X., L. Peng, D. Zheng, and J. Tao, 2008: Cloudiness variations over the Qinghai-Tibet Plateau during 1971–2004. *J. Geogr. Sci.,* **18,** 142–154, doi:10.1007/s11442-008-0142-1.

Zhao, G., and L. Di Girolamo, 2004: A cloud fraction versus view angle technique for automatic in-scene evaluation of the MISR cloud mask. *J. Appl. Meteor.,* **43,** 860–869, doi:10.1175/1520-0450(2004)043<0860:ACFVVA>2.0.CO;2.